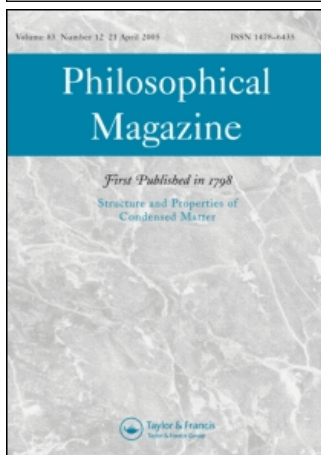


This article was downloaded by:[University of Sydney]  
On: 8 April 2008  
Access Details: [subscription number 777157964]  
Publisher: Taylor & Francis  
Informa Ltd Registered in England and Wales Registered Number: 1072954  
Registered office: Mortimer House, 37-41 Mortimer Street, London W1T 3JH, UK



## Philosophical Magazine

### First published in 1798

Publication details, including instructions for authors and subscription information:  
<http://www.informaworld.com/smpp/title~content=t713695589>

### Structural studies of disordered carbons by high-energy X-ray diffraction

L. Hawelek <sup>a</sup>; J. Kołoczek <sup>a</sup>; A. Bródka <sup>a</sup>; J. C. Dore <sup>b</sup>; V. Honkimäki <sup>c</sup>; A. Burian <sup>a</sup>

<sup>a</sup> A. Chelkowski Institute of Physics, University of Silesia, ul. Uniwersytecka 4, Katowice, Poland

<sup>b</sup> School of Physical Sciences, University of Kent, Canterbury, CT2 7NR, UK

<sup>c</sup> European Synchrotron Radiation Facility, Grenoble, France

Online Publication Date: 01 November 2007

To cite this Article: Hawelek, L., Kołoczek, J., Bródka, A., Dore, J. C., Honkimäki, V. and Burian, A. (2007) 'Structural studies of disordered carbons by high-energy

X-ray diffraction', *Philosophical Magazine*, 87:32, 4973 - 4986

To link to this article: DOI: 10.1080/14786430701594038

URL: <http://dx.doi.org/10.1080/14786430701594038>

PLEASE SCROLL DOWN FOR ARTICLE

Full terms and conditions of use: <http://www.informaworld.com/terms-and-conditions-of-access.pdf>

This article maybe used for research, teaching and private study purposes. Any substantial or systematic reproduction, re-distribution, re-selling, loan or sub-licensing, systematic supply or distribution in any form to anyone is expressly forbidden.

The publisher does not give any warranty express or implied or make any representation that the contents will be complete or accurate or up to date. The accuracy of any instructions, formulae and drug doses should be independently verified with primary sources. The publisher shall not be liable for any loss, actions, claims, proceedings, demand or costs or damages whatsoever or howsoever caused arising directly or indirectly in connection with or arising out of the use of this material.

## Structural studies of disordered carbons by high-energy X-ray diffraction

L. HAWĘLEK<sup>†</sup>, J. KOŁOCZEK<sup>†¶</sup>, A. BRÓDKA<sup>†</sup>, J. C. DORE<sup>‡</sup>,  
V. HONKIMÄKI<sup>§</sup> and A. BURIAN<sup>\*†</sup>

<sup>†</sup>A. Chelkowski Institute of Physics, University of Silesia, ul. Uniwersytecka 4,  
40-007, Katowice, Poland

<sup>‡</sup>School of Physical Sciences, University of Kent, Canterbury, CT2 7NR, UK

<sup>§</sup>European Synchrotron Radiation Facility, BP 220, 38043, Grenoble, France

(Received 15 February 2007; accepted in revised form 23 July 2007)

X-ray diffraction measurements were carried out on three samples of disordered, commercially produced carbons, AX21, CXV and BP71, on the ID15B beam-line at the European Synchrotron Radiation Facility (ESRF), Grenoble. Intensity data were converted to pair correlation functions via the Fourier transform. The results obtained show that the structure of the studied samples consists of one–four graphite-like layers, stacked without spatial correlations. The size of the ordered regions is in the range of 9–16 Å. The atomic arrangement within an individual layer can be described in terms of the paracrystalline ordering, in which lattice distortions propagate proportionally to the square root of interatomic distances. The paracrystalline structure was simulated by introducing the Stone–Wales defects (pair of two pentagons and two heptagons), randomly distributed in the network. The resulting structures were relaxed using the reactive empirical bond order potential for carbon–carbon interaction and the Lennard-Jones potential with parameters for interlayer interactions. Such defects lead to curvature of individual layers.

### 1. Introduction

In previous studies it has been demonstrated that non-crystalline forms of carbon may exist as either ‘graphitizing’ or ‘non-graphitizing’, according to the Franklin classification [1]. The so-called ‘non-graphitizing’ carbons cannot be transformed into graphite even at temperatures of 3000°C or above; they tend to be hard and low-density materials with an isotropic structure and a high proportion of porosity. Non-graphitizing carbons can develop exceptionally high surface areas after mild oxidation (or activation) and therefore are important industrial materials widely used as adsorbents, catalyst supports or in lithium batteries [2, 3]. Although these

---

\*Corresponding author. Email: andrzej.burian@us.edu.pl

¶Present address: Institute of Environmental Protection, KASHUE, ul. Kolektorska 4, 01-692 Warsaw, Poland.

materials have been known for over 60 years, their structure is not satisfactorily described at the atomic scale. A detailed knowledge of the structure of non-graphitizing carbons is important to understand the properties of these materials. In contrast, graphitizing carbons can be easily transformed into graphite by heat treatment [1].

Early studies of non-crystalline carbons have suggested two types of their structure. First is the model in which small graphitic crystallites form the disordered cross-linked structure. However, the nature of these cross-links is not precisely described [1]. In the second model offered by Warren, the graphitic planes are buckled and exist in stacks of a few layers that are arranged without spatial correlations [4]; such a separate graphitic layer is named the graphene layer. The model of this kind is called turbostratic and it was originally applied to describe the structure of carbon black. The limitations and shortcomings of these models have been reviewed by Harris [3]. Gardner *et al.* [5] suggested that this model, composed of three to four layers, describes reasonably the structure of various carbons prepared from organic precursors. Burian *et al.* [6] showed that the turbostratic model, composed of four layers with paracrystalline distortion of the hexagonal network within a single layer, accounts very well for the neutron diffraction experimental data of activated carbons produced from a polymer of phenol–formaldehyde resin. Later modelling studies of the disordered carbons produced from saccharose and anthracene provided evidence that the paracrystalline model, containing three–four layers each about 20 Å in diameter, correctly reproduces all features of the experimental neutron diffraction data in both reciprocal and real space. In this model it was assumed that: graphite layers are randomly translated and rotated, according to the turbostratic structure, the nearest-neighbour carbon–carbon distances can randomly fluctuate and the resulting network distortions propagate proportionally to the square root of the interatomic distances [7]. The discovery of fullerenes has prompted several groups to consider whether curved elements containing non-six-membered rings with  $sp^2$  bonded carbon atoms could be present in non-crystalline forms of carbon because such fullerene-like elements are now known to be highly stable [3, 8–15].

The main aim of the present study is to describe in detail the structure of the commercial activated carbons, AX21, CXV and BP71, at the atomic level using high-energy X-ray diffraction and to see whether the idea that non-hexagonal rings are present in these materials can be supported by careful interpretation of the diffraction data. Detailed characteristics of these materials can be found elsewhere [16].

## 2. Experimental

Three samples of commercially available carbons were studied: AX21, CXV and BP71. AX21 is a finely powdered petroleum pitch-based carbon, chemically activated using potassium hydroxide. CXV comes from finely powdered wood-based carbon. BP71 (Black Pearls 71) is a graphitized carbon black, having the appearance of small, spherical particles which disintegrate into smaller particles under slight pressure [16].

CXV and BP71 were activated with CO<sub>2</sub> and steam, respectively. The bulk densities of the investigated carbons are in the range 1.5–1.8 g cm<sup>-3</sup>. The micropore sizes of AX21, CXV and BP71 are 12 Å, 5–10 Å and 5 Å, respectively, whereas the mesopore sizes are 200–300 Å, 150–200 Å and 60–120 Å. The pore volumes of three samples are in the range 0.4–0.8 cm<sup>3</sup> g<sup>-1</sup>. Their BET surface areas are 2513 m<sup>2</sup> g<sup>-1</sup>, 1792 m<sup>2</sup> g<sup>-1</sup> and 1347 m<sup>2</sup> g<sup>-1</sup>. Residual hydrogen arising mainly from the activated process has been revealed in the investigated samples. Typically, the H:C ratio is of the order 4–6%.

The diffraction experiment was carried out on the ID15B beamline at the ESRF in Grenoble, France. An incident beam energy of 95.4 keV was used for recording of two-dimensional diffraction patterns using an image plate as a two-dimensional detector. The MAR on-line image plate detection system consists of 2300 × 2300 pixels, each of 0.15 mm in size. After proper integration over azimuth angles the recorded data covered  $Q$ -range up to 27 Å<sup>-1</sup>. The experimental procedures are described in detail in our previous paper [17].

### 3. Theoretical background

The samples studied in this work have a structure intermediate between amorphous and crystalline. Therefore the formalism of the radial distribution function was used to describe the structure of the investigated carbons. If we consider the diffraction process by such partly ordered systems, the distribution of intensities averaged over all orientations can be calculated from the Debye equation

$$I_N(Q) = f^2 \sum_{i=1}^N \sum_{j=1}^N \frac{\sin Qr_{ij}}{Qr_{ij}}, \quad (1a)$$

which is related to the structure factor

$$S_N(Q) = \frac{I_N(Q)}{f^2}, \quad (1b)$$

where  $Q = 4\pi \sin \theta/\lambda$  is the scattering vector,  $2\theta$  is the scattering angle,  $\lambda$  denotes the wavelength,  $N$  indicates the number of atoms,  $f$  is the atomic scattering factor of carbon and  $r_{ij}$  indicates the distance between the  $i$ th and  $j$ th atoms. The Debye equation, normalized to one atom, can be used for modelling the structure of the disordered carbons. Attenuation of the intensity due to thermal vibrations of atoms and static disorder is taken into account by the Debye–Waller-type term  $\exp(-\sigma_{ij}^2 Q^2/2)$ , where  $\sigma_{ij}$  is the standard deviation of the interatomic distances. Finally, the structure factor per one atom,  $S(Q)$ , is expressed as

$$S(Q) = 1 + \frac{1}{N} \left[ \sum_{i=1}^N \sum_{j=1}^N \frac{\sin(Qr_{ij})}{Qr_{ij}} \exp\left(-\frac{\sigma_{ij}^2 Q^2}{2}\right) \right]_{i \neq j}. \quad (2)$$

For further analysis, a real space representation of the diffraction data in the form of the reduced radial distribution function is calculated converting the structure factor by the sine Fourier transform as follows:

$$d(r) = \frac{2}{\pi} \int_0^{Q_{\max}} Q(S(Q) - 1) \sin(Qr) \frac{\sin(\pi Q/Q_{\max})}{\pi Q/Q_{\max}} dQ, \quad (3)$$

where  $Q_{\max}$  is the maximum value of the scattering vector available in the experiment and the term  $\sin(\pi Q/Q_{\max})/(\pi Q/Q_{\max})$  denotes the Lorch modification function that reduces truncation effects. In the present work, the value of  $Q_{\max} = 24 \text{ \AA}^{-1}$  was taken for computation because beyond this limit the experimental data exhibit only noisy behaviour.

Two approaches to the structure of the investigated samples were considered. In the first, the paracrystalline model is defined by the size of the ordered region, the number of layers in the stack, the values of the graphite lattice constants  $a$ ,  $c$ , the standard deviation of the interatomic distances for atoms lying in the same layer  $\sigma_{\text{intra}}$  and the standard deviation of the interlayer spacing  $\sigma_{\text{inter}}$  [6, 7]. The generalized Debye–Waller factor with  $\sigma_{\text{intra}} = \sigma_0 r^{1/2}$  and  $\sigma_{\text{inter}} = \sigma_1 (\Delta n)^{1/2}$  ( $\Delta n = n_i - n_j$ ,  $n_i$  and  $n_j$  numerate the layers), can be included assuming  $\sigma_0$  and  $\sigma_1$  as the adjustable parameters. The paracrystalline structure is based on the assumption that the distances from any atom to adjacent atoms fluctuate without statistical correlations and these fluctuations propagate proportionally to the square root of interatomic distance according to the combination law of independent probability distributions of the Gaussian type [6, 7, 18]. Such fluctuations result in distribution of the nearest-neighbour interatomic distances instead of one distance of  $1.42 \text{ \AA}$ , typical for graphite. It is essential to note that within this approach disorder was imposed on the model by the appropriate form of the generalized Debye–Waller factor.

In the second approach, the paracrystalline structure was generated assuming defects in the form of two pentagon–heptagon pairs, which are randomly distributed over the graphene network. Such defects are generated by rotating a randomly chosen C–C bond, according to the Stone–Wales mechanism [19]. The generated atomic models were then relaxed by minimizing their energy using the reactive empirical bond order (REBO) potential for atoms lying within a layer [20] and the Lennard-Jones potential for interlayer interactions [21]. A conjugated gradients algorithm was employed for the minimization procedure. The binding energy of carbon atoms is described as follows

$$E_b = \sum_i \sum_{j>i} f_c(r_{ij}) [V_R(r_{ij}) - b_{ij} V_A(r_{ij})], \quad (4)$$

where  $r_{ij}$  is a distance between atom  $i$ th and  $j$ th,  $f_c(r_{ij})$  denotes the switching function, the value of which is equal to one for the nearest neighbours and is equal to zero for other distances. The summation procedure is carried out over the nearest neighbours.  $V_R(r_{ij})$  and  $V_A(r_{ij})$  represent interatomic repulsion and attraction from valence electrons, respectively. The bond-order function,  $b_{ij}$ , depends on the local coordination and the bond angles for the atoms, that leads to realistic description of energies and lengths of C–C single, double and triple bonds [20]. Therefore, periodic boundary conditions are not necessary to take into account discontinuity of

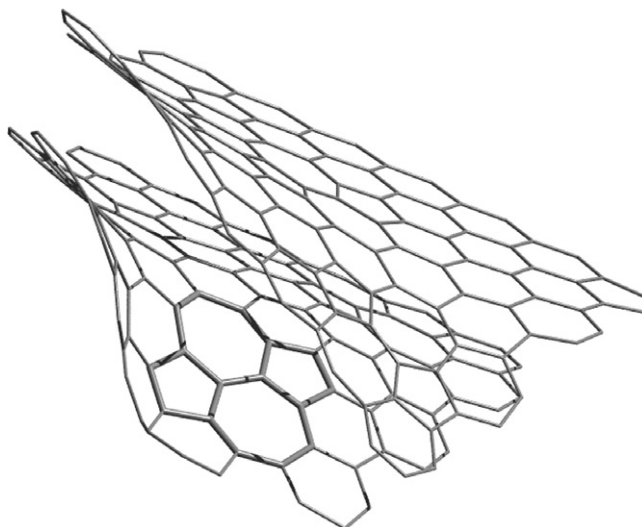


Figure 1. The relaxed double-layer model with the Stone–Wales defects. One defect (two pentagons and two heptagons) is shown as thick lines.

the constructed models at their edges during the energy minimization procedure. The presence of pentagons and heptagons leads to the distribution of the interatomic distances as it has been assumed in the paracrystalline model. In figure 1, the Stone–Wales defect is shown as an example. Such a procedure leads to the construction of the real model in space with intrinsic disorder.

#### 4. Results and discussion

For the sets of the Cartesian coordinates the interatomic distances were calculated, yielding the structure factor  $S(Q)$ , according to equation (2). From the structure factors the reduced radial distribution functions were then computed using equation (3). For the activated carbon AX21, in the first step of modelling, the paracrystalline theory was applied in which the paracrystalline distortion is introduced by applying the generalized Debye–Waller factor as described above in section 3. The amplitude of the first diffraction peak, appearing at about  $1.75 \text{ \AA}^{-1}$ , depends on a number of layers [6]. For the AX21 carbon this peak has a low intensity, which suggests that the number of the layers is small. In order to correctly reproduce this peak the model consisting of a mixture of one-layer and two-layer atomic arrangements in proportion 30% and 70%, respectively, has been constructed. In principle one can construct the model containing more layers (three or four), which correctly reproduces the experimental data both in reciprocal and real space, but in such a case its contribution has to be lower than 70%. Playing with the number of layers one increases the number of free parameters of the model, and therefore the simplest model consisting of one–two layers is considered. The model of  $16 \text{ \AA}$  in size with the value of the standard deviations of the interatomic

distances  $\sigma_0 = 0.06 \text{ \AA}$  has proved to be optimal to reproduce properly all features of the structure factor and the reduced radial distribution function. The interlayer spacing was approximately  $3.6 \text{ \AA}$  with the value of  $\sigma_1 = 0.03 \text{ \AA}$ . For the double-layer arrangement the interlayer paracrystalline disorder was introduced generating 100 statistically independent sets of the atomic arrangements with Gaussian distribution of the interlayer spacing, generated by a suitable numerical procedure [7].

The procedure employed to generate a series of random numbers with the Gaussian distribution is based on the central-limit theorem. First the random variables  $X_i$  with uniform distribution over the  $[0;1]$  range were generated using a standard FORTRAN routine and then the variables  $X_G(0;1)$  with the Gaussian distribution and the mean value 0 and the standard deviation 1 were computed according to

$$X_G(0; 1) = \frac{(\sum_{i=1}^n X_i - (n/2))}{\sqrt{n/12}}. \quad (5)$$

In the present work, the value of  $n = 200$  was taken for computation. Finally, the variables obtained were scaled,  $X_G(\mu; \sigma) = X_G(0;1)\sigma + \mu$ , to obtain random variables with a Gaussian distribution and a mean value  $\mu$  and standard deviation  $\sigma$ . Such generated interlayer spacings reproduced well the Gaussian distribution. The structure factor was calculated for each set of the generated atomic arrangements. The final structure factor was computed by averaging over all the individual structure factors. The same procedure was used for other samples. The numbers of atoms in the one- and double-layer arrangements were 112 and 231, respectively. The calculated and experimental structure factors are compared in figure 2.

In the next step, the Stone–Wales defects were generated for the one-layer set consisting of 112 atoms and for the 231 atom double-layer set, keeping the 30%/70% proportion between them. The distance independent Debye–Waller factor,  $\sigma = 0.07 \text{ \AA}$ , was taken for computation. In the one-layer arrangement, the number of the pentagon/heptagon pairs was four and in the case of the double-layer arrangement there were eight such pairs. After relaxation of the generated models the structure factors were calculated and averaged according to the 30%/70% proportion. The resulting structure factor is shown in the top part of figure 2.

From inspection of figure 2 it can be seen that the experimental structure factor is satisfactorily reproduced by both calculation procedures using paracrystalline and defect-based modelling. It should be noted that the model containing defects properly attenuates the structure factor and leads to practically the same effects as the paracrystalline model. These findings are reinforced by analysis of the data in real space. The experimental and computed reduced radial distribution functions, shown in figure 3, are in a reasonable agreement. Peak positions are well reproduced by the models; however, slight discrepancies in their amplitudes are easily seen. In particular, the reduced radial distribution function computed for the model with the Stone–Wales defects is attenuated too much compared with the paracrystalline model, which seems to better fit the experimental function.

A similar procedure was applied to the activated carbon CXV. The experimental structure factors are displayed in the bottom part of figure 4. The first diffraction peak, observed at  $Q = 1.85 \text{ \AA}^{-1}$ , is clearly higher than that of

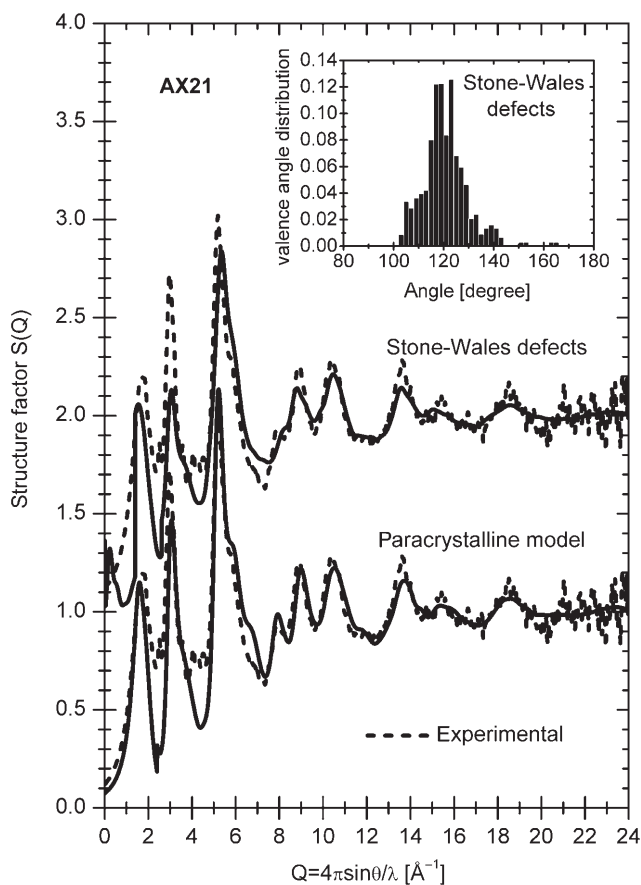


Figure 2. Comparison of the experimental structure factors with those of the paracrystalline model and the relaxed model with the Stone–Wales defects for the activated carbon AX21.

the AX21 sample. Moreover, the higher- $Q$  oscillations are apparently more damped for CXV. It means that the number of layers for the CXV carbon is higher and this sample is more disordered, as far as the atomic arrangement within a single layer is concerned. The structure of this sample was described by the paracrystalline double-layer model of  $9 \text{\AA}$  in size, containing 79 carbon atoms. The interlayer spacing  $3.4 \text{\AA}$ , the standard deviations  $\sigma_0 = 0.075 \text{\AA}$  and  $\sigma_1 = 0.03 \text{\AA}$  were taken for computations. The model with the Stone–Wales defects consisted of 79 carbon atoms with three pentagon/heptagon pairs. The simulation results for both models are compared with the experimental data in figures 4–5. The overall agreement between the simulations and the experiment is good. The only difference is that the first reduced radial distribution peak at about  $1.42 \text{\AA}$  for the model with non-hexagonal defects is apparently higher than those of the paracrystalline model and the experimental function. It is important to note that the nearest-neighbour peak of the experimental reduced radial distribution function for CXV is apparently lower than that of AX21. This finding is consistent with the size of the assumed values of individual layers in

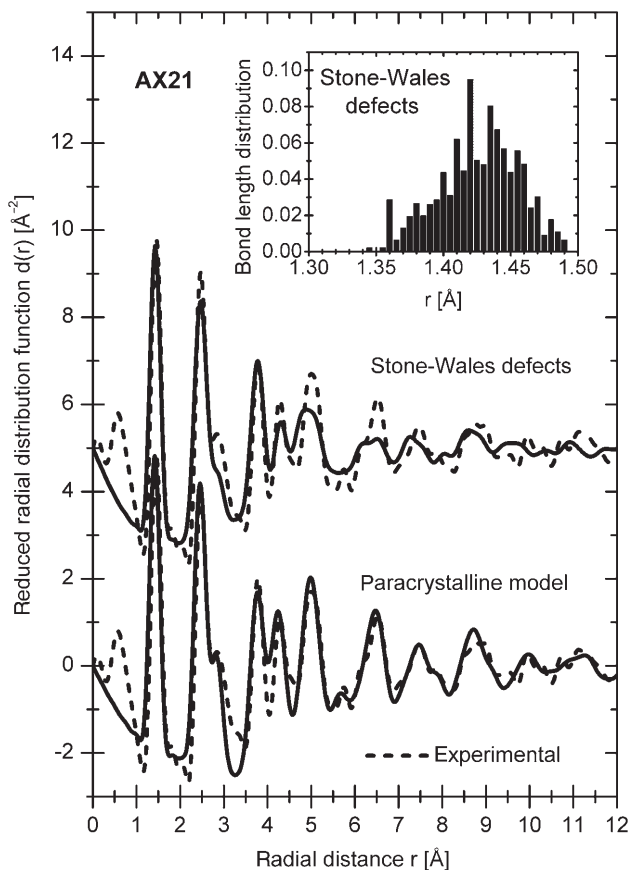


Figure 3. Comparison of the experimental reduced radial distribution functions with those of the paracrystalline model and the relaxed model with the Stone–Wales defects for the activated carbon AX21.

both models. The amplitude of this peak is related to the number of the nearest neighbours, which should be lower for the model with a smaller size because in such a case proportion of atoms lying at the edges of the graphene layer is higher and these atoms have lower coordination.

A paracrystalline model of 16 Å in size, consisting of 293 carbon atoms arranged within the stack of four layers, was assumed for the BP71 activated carbon. The higher number layers was necessary to correctly reproduce the first diffraction line. The value of the Debye–Waller parameter  $\sigma_0 = 0.062 \text{ \AA}$ . The interlayer distance 3.4 Å and  $\sigma_1 = 0.045 \text{ \AA}$  were found to be optimal to satisfactorily reproduce the profile of the first diffraction peak. The model with the Stone–Wales defects contained the same number of atoms as the paracrystalline model and 15 pentagon/heptagon pairs. Comparisons of the computed structure factors and the reduced radial distribution functions with the experimental data are shown in figures 6–7. The agreement between the simulated and experimental functions is good. However, apparent discrepancies between the experimental and simulated structure

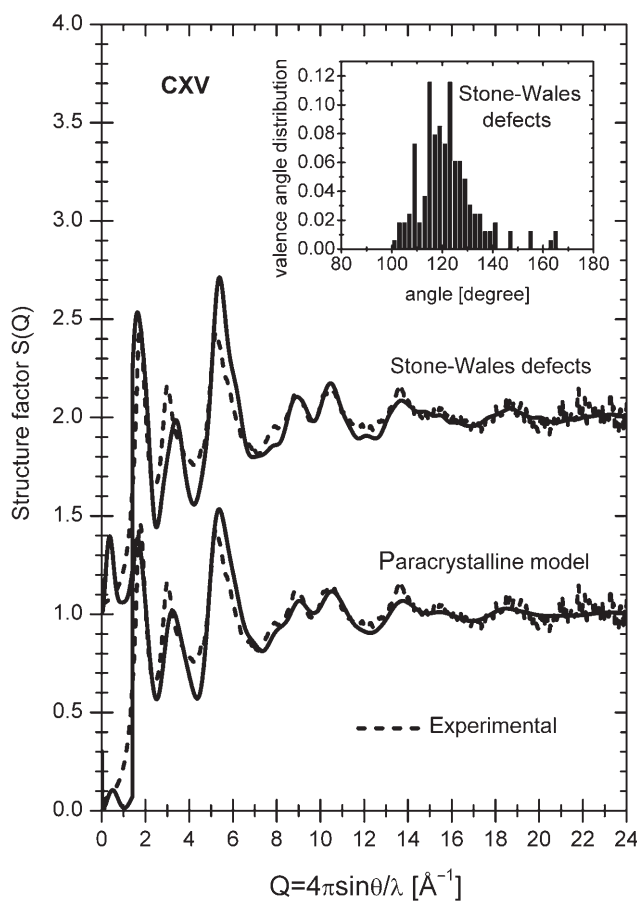


Figure 4. Comparison of the experimental structure factors with those of the paracrystalline model and the relaxed model with the Stone–Wales defects for the activated carbon CXV.

factors can be seen at about  $3 \text{\AA}^{-1}$  and the paracrystalline model better fits the experimental reduced radial distribution function than the model with the Stone–Wales defects.

In figures 2–7, the distributions of the valence angles and the bond lengths are shown in the insets. The valence angle and bond length distributions show that in the models containing the Stone–Wales defects the generated atomic arrangements deviate from the perfect hexagonal arrangement, as can be seen in figure 8, in which the models are displayed. The originally flat graphene sheets are transformed into curved structures during the energy relaxation procedure using the above-described potentials. Curvature of the sheets is clearly related to the presence of the non-hexagonal rings, i.e. pentagons and heptagons. The same number of five- and seven-membered rings allows the turbostratic structure to be retained because the occurrence of pentagons leads to positive curvature, whereas heptagons cause negative curvature, which facilitates turbostratic layering. Curvature in the case of the CXV carbon is apparently smaller because of a lower concentration of defects.

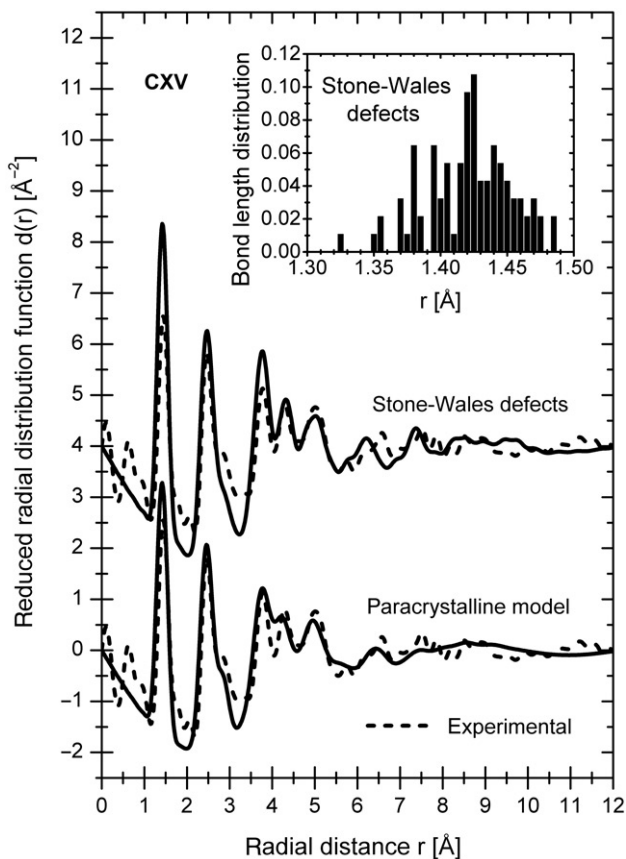


Figure 5. Comparison of the experimental reduced radial distribution functions with those of the paracrystalline model and the relaxed model with the Stone–Wales defects for the activated carbon CXV.

Valence angles less than  $120^\circ$  are observed in pentagons and at adjacent pentagon–hexagon pairs, whereas the angles are greater than  $120^\circ$  in heptagons and at edges of the models. The nearest-neighbour interatomic distances shorter than  $1.42 \text{ \AA}$  are related to C=C double bonds, whereas the bond lengths longer than this value results from single bonding. In all the models the bond lengths are seen to involve a wide range of interatomic distances, centred on the  $1.42 \text{ \AA}$  value characteristic for graphitic bonding.

In summary, it is essential to point out that the constructed models consist of building structural units containing one to four layers and that the Debye–Waller type factor is introduced to account for atomic disorder. In the paracrystalline models, disorder increases with the square root of the interatomic distances due to their fluctuations. The models containing the Stone–Wales defects reasonably reproduce these fluctuations. These models should be regarded as average and simplified representations of the real structure. As the investigated carbons are highly porous it is expected that small-angle scattering due to micropores contributes to the structure factors in their low- $Q$  regions. Such a contribution related to

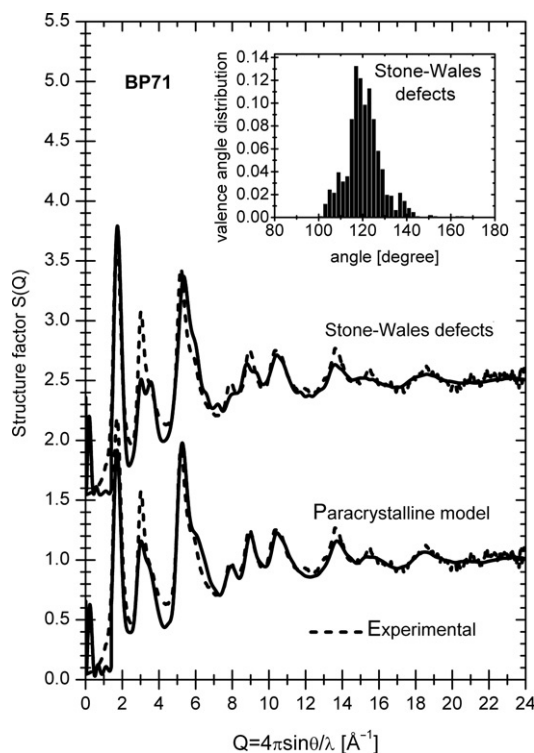


Figure 6. Comparison of the experimental structure factors with those of the paracrystalline model and the relaxed model with the Stone–Wales defects for the activated carbon BP71.

cross-correlations between different structure units may lead to discrepancies between the experimental and calculated structure factors, as seen in figures 2 and 6. Moreover, the presence of other structural elements cannot be ruled out. The occurrence of five-membered rings, not accompanied by heptagons, has been considered. Pentagons produce strong local curvature of the graphene sheet, which can even lead to closed cages and fullerene-like structures, as has been observed in non-graphitizing carbons by high-resolution transmission electron microscopy [8, 9, 13]. But in such a case it is impossible to retain turbostratic stacking for the multilayer models [14]. Also, the presence of  $sp^3$ -type defects can be expected in activated carbons, as suggested in the literature [16, 22]. In modelling studies, such local structural variability can be included to a certain degree, but in general the present data cannot provide direct evidence for their presence.

## 5. Conclusions

High-energy X-ray diffraction has proved to be an efficient tool for studies of disordered activated carbons. The applied interpretation methods, based on the paracrystalline concept and the assumption about the presence of non-hexagonal

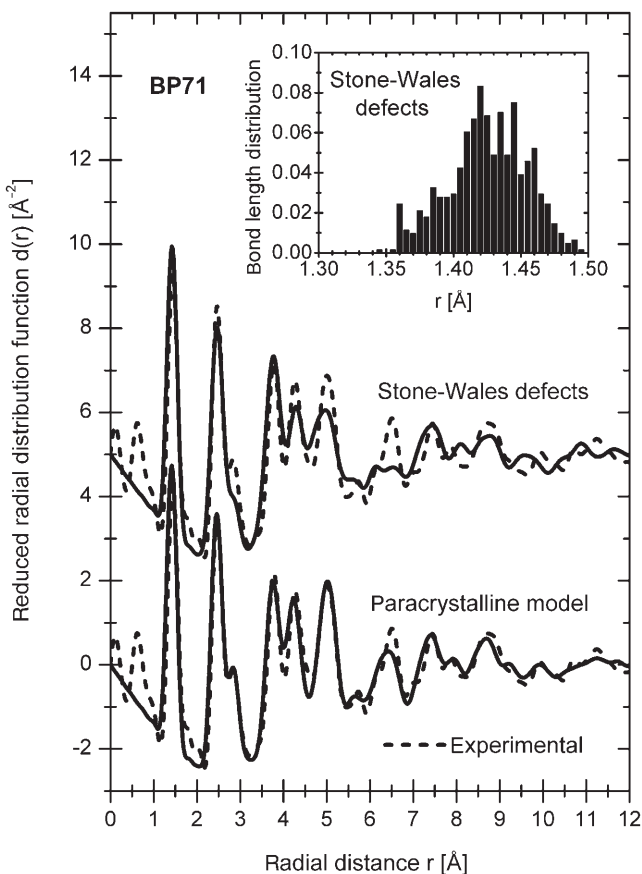


Figure 7. Comparison of the experimental reduced radial distribution functions with those of the paracrystalline model and the relaxed model with the Stone–Wales defects for the activated carbon BP71.

rings in the investigated carbons lead to adequate description of the atomic arrangement in these materials, which is in reasonable agreement with the experimental data in reciprocal and real space. It is essential to note that the paracrystalline structure of the materials in question can be related to the presence of pentagons and heptagons. The carbon–carbon distances in pentagons and heptagons have different lengths than that of graphite. If these interatomic distances are randomly distributed over the network, the paracrystalline distortion of the structure is generated and the resulting layers are curved. As has been reported elsewhere [16], the AX21, CXV and BP71 carbons are highly porous, non-graphitizing materials. The porosity and resistance of these carbons to graphitization have been related to the presence of fullerene- or nanotube-like fragments as building elements of carbonaceous materials [3, 8–11, 13]. Their presence has been revealed using high-resolution transmission microscopy and Raman spectroscopy. In the present paper, it has been shown that the high-energy X-ray diffraction method accompanied by the computer generation and the subsequent energy

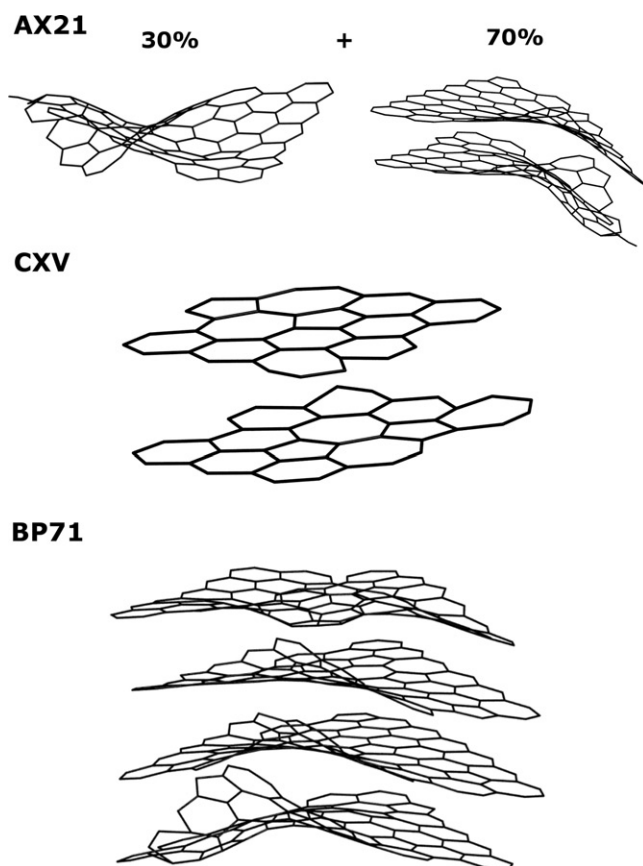


Figure 8. The relaxed models of the structure for the AX21, CXV and BP71 carbons.

relaxation proved to be the effective tool for testing the validity of various structural models of activated carbons. After the discovery of fullerenes in 1985 and nanotubes in 1991, we now know that carbons containing non-six-membered rings can form highly stable structures. The present work supports this point of view by providing experimental evidence that curved elements may be formed in activated carbons during a preparation and that they are not transformed into the perfect graphite structure upon subsequent heat treatment. Such fragments have been found in the models with the Stone–Wales defects, as shown in figure 8.

### Acknowledgement

We would like to thank Dr A. Szczygielska from the University of Silesia for participation in the experiment.

**References**

- [1] R.E. Franklin, Proc. R. Soc. A **209** 196 (1951).
- [2] M. Smisek and S. Cerny, *Active Carbon* (Elsevier, Amsterdam, 1970).
- [3] P.J.F. Harris, Int. Mater. Rev. **42** 206 (1997).
- [4] B.E. Warren, Phys. Rev. **19** 693 (1941).
- [5] M.A. Gardner, J.C. Dore, A.N. North, *et al.*, Carbon **34** 857 (1996).
- [6] A. Burian, A. Ratuszna, J.C. Dore, *et al.*, Carbon **36** 1613 (1998).
- [7] A. Szczygielska, A. Burian and J.C. Dore, J. Phys. Condensed Matter **13** 5545 (2001).
- [8] P.J.F. Harris and S.C. Tsang, Phil. Mag. A **76** 667 (1997).
- [9] P.J.F. Harris, A. Burian and S. Duber, Phil. Mag. Lett. **80** 381 (2000).
- [10] A. Burian and J.C. Dore, Acta phys. Polonica A **98** 457 (2000).
- [11] A. Burian, P. Daniel, S. Duber, *et al.*, Phil. Mag. B **81** 525 (2001).
- [12] A. Burian, A. Szczygielska, J. Koloczek, *et al.*, Acta Phys. Polonica A **101** 751 (2002).
- [13] P.J.F. Harris, Phil. Mag. **84** 3159 (2004).
- [14] M.A. Smith, H.C. Foley and R.F. Lobo, Carbon **42** 2041 (2004).
- [15] T. Petersen, I. Yarovsky, I. Snook, *et al.*, Carbon **42** 2457 (2004).
- [16] M.A. Gardner, Structural characterization of porous carbons using scattering techniques. PhD thesis, University of Kent (1995).
- [17] L. Hawelek, J. Koloczek, A. Burian, *et al.*, J. Alloys Compounds **401** 51 (2005).
- [18] A.M. Hindeleh and R. Hosemann, J. Macromol. Sci. Phys. B **34** 327 (1995).
- [19] A. Stone and D.J. Wales, Chem. Phys. Lett. **128** 501 (1996).
- [20] D.W. Brenner, O.A. Shenderova, J.A. Harrison, *et al.*, J. Phys. Condensed Matter **14** 783 (2002).
- [21] L.A. Girifalco, M. Hodak and R.S. Lee, Phys. Rev. B **62** 13104 (2000).
- [22] V. Petkov, R.G. DiFrancesco, S.J.L. Billinge, *et al.*, Phil. Mag. B **79** 1519 (1999).